

The Intermediate Line Region and the Baldwin Effect

M. S. Brotherton

*Institute of Geophysics and Planetary Physics, Lawrence Livermore
National Laboratory*

Paul J. Francis

*Mt Stromlo & Siding Spring Observatory and Department of Physics
and Theoretical Physics, Australian National University*

Abstract.

Statistical investigations of samples of quasars have established that clusters of properties are correlated. The strongest trends among the ultraviolet emission-line properties are characterized by the object-to-object variation of emission from low-velocity gas, the so-called “intermediate-line region” or ILR. The strongest trends among the optical emission-line properties are characterized by the object-to-object variation of the line intensity ratio of [O III] λ 5007 to optical Fe II. Additionally, the strength of ILR emission correlates with [O III]/Fe II, as well as with radio and X-ray properties. The fundamental physical parameter driving these related correlations is not yet identified. Because the variation in the ILR dominates the variation in the equivalent widths of lines showing the Baldwin effect, it is important to understand whether the physical parameter underlying this variation also drives the Baldwin effect or is a primary source of scatter in the Baldwin effect.

1. Introduction

The optical/ultraviolet spectra of quasars are similar over a wide range of luminosities and radio properties. The spectra are characterized by strong continuum emission, broad ($\Delta v > 2000 \text{ km s}^{-1}$) emission lines arising from a broad-line region (BLR), and narrow emission lines ($\Delta v < 1000 \text{ km}^{-1}$) arising from a more extended narrow-line region (NLR). Early photoionization models of the BLR (e.g., Baldwin & Netzer 1978; Kwan & Krolik 1981) showed that it was possible to reproduce typical BLR line ratios with a single type of AGN cloud (standard model reviewed and critiqued by, e.g., Ferland 1986), but it is clear that the BLR is heterogeneous: (1) high and low-ionization lines are underpredicted by the standard model (e.g., Netzer 1985), (2) lines show ionization-dependent velocity shifts (Gaskell 1982; Espey et al. 1989, 1994), (3) different lines show different time lags in response to continuum changes (e.g., Korista et al. 1995), (4) different lines can show dramatic profile differences (e.g., Netzer et al. 1994). The fact that single-zone models work as well as they do can be attributed to the powerful selection effects of “locally optimally emitting clouds” (Baldwin et

al. 1995; Ferland this volume); many emission lines in the optical and ultraviolet are preferentially emitted from clouds with a narrow range of properties.

Even if beset by strong selection effects that dominate its emissions, the BLR is still an important probe of the spatially unresolvable sub-parsec environment of quasars. Gas to fuel the presumed supermassive black hole central engine must pass through the BLR, as must ISM and IGM-enriching outflows originating in disk winds or jets. Statistical relationships among broad-line and other properties provide a means of investigating physical parameters, such as the black hole mass and accretion rate, that underlie the appearance of quasars. As the size of carefully selected quasar samples grows, as well as the quality of data available for such samples, likewise grows the need for more sophisticated statistical techniques.

One such multivariate technique that has become increasingly applied in AGN studies and other areas of astrophysics is principal component analysis or PCA (e.g., Bernstein 1988). Technically, PCA is the eigenanalysis of the correlation matrix of a set of input variables; the results are the eigenvectors (or principal components) and their corresponding eigenvalues. The eigenvectors can be visualized as the directions in parameter space described by the elliptical axes of the scatterplot of input variables, and the eigenvalues as a quantification of the amount of variance in the direction of these axes. Eigenvector 1 is then the direction in n -dimensional parameter space that accounts for the most variation in the data set, and can include correlations among many variables. When PCA is effective, the many input variables (typically measured properties that would a priori seem unrelated) can be transformed into a few eigenvectors that may be interpreted as the effect of the important underlying physical processes.

The discussion that follows describes eigenvector 1 correlations in the ultraviolet and optical spectra of quasars, how they are related to each other and other quasar properties, what physics underlies eigenvector 1, and how all of this is related to the Baldwin effect. The primary source of variance in the ultraviolet spectra of quasars involves the equivalent widths of the emission lines, which is one of the components of the Baldwin effect. If eigenvector 1 is luminosity independent (points in a direction orthogonal to luminosity), then the physical parameter underlying eigenvector 1 is the source of scatter in the Baldwin effect. If eigenvector 1 depends on luminosity (points in a direction parallel to luminosity), then the physical parameter underlying eigenvector 1 helps create the Baldwin effect. As will be discussed, current data sets provide contradictory evidence for which is the case.

2. Ultraviolet Eigenvector 1: The Intermediate Line Region

Investigations of luminous quasars' broad UV lines identified strong correlations involving emission-line widths, shifts, equivalent widths, and ratios (Francis et al. 1992; Wills et al. 1993; Brotherton et al. 1994a, b). A simple model developed to explain these trends approximates UV broad lines as emission from two regions, an intermediate-line region (ILR), and a very-broad-line region (VBLR), together comprising the traditional BLR.

This decomposition is a simple, approximate explanation for the observation that broader lined quasars have smaller equivalent widths and different line

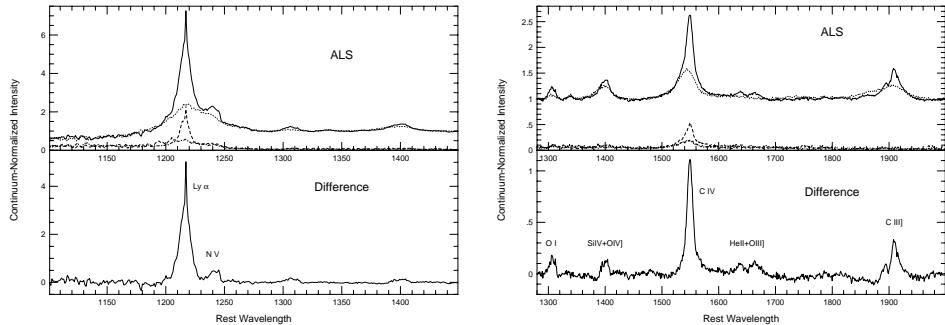


Figure 1. The narrow (*solid*) and broad-lined (*dotted*) continuum-normalized (“EW”) composite spectra of the Ly α region (left) and C IV (right). The difference spectra are displayed below. From Brotherton et al. 1994b.

ratios when compared to narrower lined quasars. Figure 1 illustrates this using a composite of narrow-lined quasar spectra ($2000 \text{ km s}^{-1} < \text{FWHM}_{CIV} < 3500 \text{ km s}^{-1}$) and a composite of broad-lined quasar spectra ($6000 \text{ km s}^{-1} < \text{FWHM}_{CIV} < 8000 \text{ km s}^{-1}$). The difference spectrum, or ILR spectrum, produced this way is essentially identical to the first principal component (PC1) spectrum produced by the spectral PCA of the Large Bright Quasar Survey (Brotherton et al. 1994b; Francis et al. 1992).

2.1. Photoionization Modeling

The emission-line ratios of the ILR (difference) spectrum and the VBLR (broad-lined composite) can be modeled using photoionization codes such as CLOUDY (Ferland 1993). While single-zone models fail to reproduce the highest and lowest ionization lines, a two-zone model does a better job reproducing the heterogeneous BLR. Brotherton et al. (1994b) showed that the ILR spectrum could be well modeled, whereas the VBLR spectrum is probably still too heterogeneous for a good single-zone model. The discriminating diagnostic lines are O III] $\lambda 1663$, a semi-forbidden line, and Al III $\lambda 1860$, an important coolant in high density clouds, which suggest that the ILR is more distant from the nucleus and less dense than the rest of the BLR. The observed and derived properties of the ILR, VBLR, and the NLR are tabulated (from Brotherton et al. 1994b).

Table 1. Comparison of Emission-Line Regions

Property	NLR	ILR	VBLR
Velocity Dispersion (km s^{-1})	~ 500	~ 2000	~ 7000
Radial Distance (pc)	10^{2-3}	~ 1	~ 0.1
Gas Density (n_H, cm^{-3})	10^{4-6}	$\sim 10^{10}$	$\sim 10^{12.5}$
Ionization Parameter ($U = \phi_i/n_H$)	~ 0.01	~ 0.01	~ 0.01
Redshift cf. Systemic (km s^{-1})	0	~ 0	~ -1000
Covering Factor ($\Omega/4\pi$)	≤ 0.02	≤ 0.03	~ 0.24

Keep in mind that these results were obtained by modeling spectra derived from the most luminous quasars known, and at least the size scales can be expected to vary with luminosity (e.g., Kaspi et al. 1996).

This two-component BLR breakdown may be generalized to n -components as strong selection effects permit an ensemble of clouds experiencing a very wide range of physical conditions to reproduce, not badly, a typical quasar spectrum (Baldwin et al. 1995). The designations of “ILR” and “VBLR,” and more specifically the ratio of ILR to VBLR emission, may simply represent the limits of such an ensemble distribution. Differences in the relative emission of these limits account for much of the diversity of broad-line profiles, as well as relations among line strength, line width, asymmetry and peak blueshift.

Comparison with other AGN emission-line regions shows that the ILR spectrum tends to be intermediate between that of the VBLR and that of gas more distant from the ionizing continuum, such as the NLR and extended Ly α neb- ulosity. This suggests that the ILR may be more properly identified as an inner extension of the NLR rather than as a component of the BLR, a hypothesis strengthened below (§ 4).

3. Optical Eigenvector 1: The Fe II – [O III] Anti-Correlation

The object-to-object variation in the optical spectra of low-redshift quasars is dominated by the inverse correlation between narrow [O III] $\lambda 5007$ (FWHM $\sim 500 \text{ km s}^{-1}$) and optical Fe II emission (eigenvector 1 of the PCA of Boroson & Green 1992 of the parameterized spectra of optically selected quasars from the Bright Quasar Survey, or BQS). Figure 2 illustrates this trend. It is important to note that it is not just the equivalent width (EW) of [O III] $\lambda 5007$ involved in the correlation, but also the luminosity of [O III] $\lambda 5007$. There are a number of secondary properties also correlated with eigenvector 1: quasars with prominent [O III] $\lambda 5007$ and weak optical Fe II preferentially have broad, red-asymmetric $H\beta$ and are radio-loud and strong in hard (2 keV) X-rays (e.g., Corbin 1993). Furthermore, Laor et al. (1997), using a complete subset of the PG quasars, found that the soft X-ray spectral slope, α_x , is strongly correlated with [O III]/Fe II in the sense that strong Fe II emitting objects have steep soft X-ray spectra (the extreme of these are identified with the narrow-line Seyfert 1 objects).

4. The “Unified” Eigenvector 1

In order to study simultaneously the statistical behavior of both optical and ultraviolet spectral properties, it is necessary to observe a wide range of wave- lengths: for low-redshift quasars, the optical and the ultraviolet; for high-redshift quasars, the optical and the near-infrared. This has only recently become pos- sible with the same data quality as in the optical because of the Hubble Space Telescope (HST) and new generations of near-IR detectors.

Brotherton (1996b) obtained near-IR spectra of the $H\beta$ –[O III] $\lambda 5007$ region for 32 intermediate to high redshift quasars with a range in ILR strengths. The strength of narrow-line emission, characterized by [O III] $\lambda 5007$ relative to the

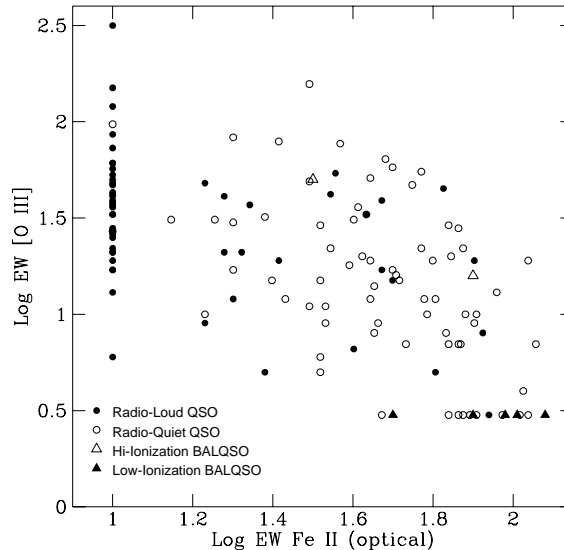


Figure 2. Low-redshift quasars, after Fig. 2 of Wills & Brotherton (1996). EWs are restframe Å. $\text{Log EW}[\text{FeII}] = 1$ are $\sim 1.5\sigma$ upper limits. $\text{Log EW}[\text{OIII}] = 0.5$ are $\sim 3\sigma$ upper limits. Low-ionization BALQSOs show excessive Fe II and negligible [O III] $\lambda 5007$ emission.

continuum and $H\beta$, is indeed correlated with that of the line cores¹ of C IV and C III], and inversely correlated with optical Fe II emission. Eigenvector 1 in the optical and the ultraviolet is the same. This result is corroborated by Wills et al. (this volume), who obtained HST ultraviolet spectra of a subsample of the BQS.

Marziani et al. (1996) and Wang et al. (1996—based on IUE data) find that the strength of optical Fe II multiplets is inversely related to the equivalent width of C IV $\lambda 1549$. This is consistent with our result that the ILR emission (which is the main determinant of EW C IV, Wills et al. 1993), is inversely correlated with optical Fe II emission. Thus the relationships among ILR, NLR, and the Fe II emission appear to hold in lower redshift, lower luminosity quasars. Table 2 summarizes a large but not exhaustive set of correlated properties that together comprise a “unified” eigenvector 1. If these quantities related by eigenvector 1 can be understood in terms of the underlying physics, their variance might constitute a “fundamental plane” for quasars by analogy with the “fundamental plane” for galaxies. Therefore understanding eigenvector 1 may allow important physical parameters to be estimated on the basis of a few easy-to-measure observables.

4.1. Physical Explanations

There is as yet no generally accepted cause for the eigenvector 1 variance. The large number of related properties poses a special problem as well as an oppor-

¹The term “line core” refers to the ILR contribution alone, not simply the emission within some velocity interval of the peak.

Table 2. Correlated Eigenvector 1 Properties

Weak ILR	Strong ILR	Ref.
Broad Ly α , C IV, C III]	Narrow Ly α , C IV, C III]	1, 2, 3, 4
Small EW C IV	Large EW C IV	1, 2
Small EW Ly α	Large EW Ly α	1, 4
Small Ly α /C IV	Large Ly α /C IV	1, 4
Large C IV/ λ 1400 Feature	Small C IV/ λ 1400 Feature	2
“Flat-topped” C IV	“Sharply Peaked” C IV	1, 2
C IV and C III] Blueshifted	C IV and C III] at Systemic z	3
Weak [O III] λ 5007	Strong [O III] λ 5007	5, 6
Strong Optical Fe II	Weak Optical Fe II	5, 6
Weak Radio-jets (Radio-quiet)	Strong Radio-jets (Radio-loud)	3, 5, 6, 7
Steep Soft-X-ray Slope	Flat Soft-X-ray-Slope	8
Small Hard X-ray Luminosity	Large Hard X-ray Luminosity	6, 8, 9, 10
Small [O III] λ 5007 Luminosity	Large [O III] λ 5007 Luminosity	6
Narrow H β with Blue Wing	Broad H β with Red Wings	6, 8
Mg II BALQSOs	no Mg II BALQSOs	11, 12

REF. 1=Francis et al. 1992. 2=Wills et al. 1993. 3=Brotherton et al. 1994a. 4=Brotherton et al. 1994b. 5=Brotherton 1996b. 6=Boroson & Green 1992. 7=Francis et al. 1993. 8=Laor et al. 1994, 1997. 9=Corbin 1993. 10=Green 1998. 11=Boroson & Meyers 1992. 12=Wills & Brotherton 1996.

tunity. Simple explanations are likely to fail because these properties represent conditions on all size scales associated with the AGN phenomenon. For instance, while the soft X-ray slope and ionizing continuum correlate with eigenvector 1 (e.g., Laor et al. 1997), this alone cannot explain the extreme range in [O III] λ 5007 equivalent width, although it might explain some of the line ratio differences (e.g., Mushotsky & Ferland 1984; Korista this volume). While radio-loudness correlates with eigenvector 1, the trends appear to hold for radio-quiet samples alone, so this property is unlikely to be fundamental. Rather we are faced with developing an explanation for some aspects of eigenvector 1 directly, and others more indirectly. A few possibilities include:

Orientation. The framework of orientation can explain the variation of many of the eigenvector 1 properties, and probably contributes to the observed correlations. The line intensity ratio of optical Fe II to [O III] λ 5007 is larger in core-dominant quasars than in lobe-dominant quasars (e.g., Zheng & O’Brien 1990; Jackson & Browne 1991; Brotherton 1996a), radio-loud classes believed to differ because of their orientation to our line of sight (e.g., Orr & Browne 1982; Wills & Brotherton 1995). The line width and asymmetry of H β also vary with core dominance (Wills & Browne 1986; Brotherton 1996a). Often these trends have been explained in terms of anisotropic line and axisymmetric continuum emission (Jackson et al. 1989; Jackson & Browne 1991). Others have invoked accretion disks as the source of the strong, possibly anisotropic Fe II emission (e.g., Collin-Souffrin, Hameury, & Joly 1988; Kwan et al. 1995). Hard X-ray

emission may also vary consistently with inclination (“face-on” implies smaller 2 keV flux) if the hard X-rays are produced by Comptonization by nonthermal electrons above an accretion disk (Ghisellini et al. 1991).

Orientation appears to fall short in accounting for at least one key item: [O III] λ 5007 luminosity. Boroson & Green (1992) argued against orientation because the luminosity of [O III] λ 5007, which they took to be an isotropic property (Jackson et al. 1989), correlated with eigenvector 1, and this was inconsistent with the strong correlation between continuum luminosity (enhanced for “face-on” quasars in the beaming model, thus decreasing EW [O III] λ 5007) and [O III] λ 5007 luminosity.

An extrapolation of the results of Baker (1997) may provide a boost for orientation, however. Baker finds, for a large sample of low-radio-frequency-selected quasars, evidence for aspect-dependent extinction from dust toroidally distributed between the BLR and NLR. Trends of the Balmer decrement and optical slope with core dominance are consistent with this interpretation. At large angles, [O III] λ 5007 emitting clouds may be partially obscured. But it is not clear if the obscuration is enough to explain the range in observed luminosity.

Orientation may be involved in driving eigenvector 1, but if so, it requires several elements including beaming effects, dust reddening, and selection biases.

Eddington Fraction. The Eddington fraction is the ratio between the luminosity of an accreting mass and its Eddington luminosity (the point at which radiation pressure balances gravity for accreting material). Laor et al. (1997), following the suggestion that steep α_x quasars are analogous to ‘high’-state Galactic black hole candidates (e.g., White, Fabian, & Mushotsky 1984; Pounds, Done, & Osborne 1995), explained the α_x vs. FWHM H β correlation in terms of range of Eddington fraction: for a given luminosity “narrow” broad lines (i.e., H β) imply a higher Eddington fraction if the line width is gravitational. An additional point in favor of this interpretation is that a steep soft α_x is predicted to arise from a weaker hard X-ray component, and for the *ROSAT*-observed sample of Laor et al. (1997), it does appear to be changes in the hard X-rays leading to changes in α_x . Also see Wandel & Boller (1998).

Boroson & Green (1992) also argued that the Eddington fraction was the important parameter. They surmised that optical Fe II emission was dependent on the covering fraction of the BLR, and that more BLR clouds (and hence higher accretion rate) would obscure the more distant NLR. Thus the covering fraction increases from the radio-loud strong [O III] λ 5007, weak Fe II quasars to the radio-quiet weak [O III] λ 5007, strong Fe II quasars. They also noted that PG 1700+518, a broad absorption line quasar or BALQSO, is found at the high covering fraction end.

Age. This explanation is related to the above in the details, but is more fundamental. Sanders et al. (1988) proposed a scenario in which galaxy mergers produce dust-rich ultraluminous infrared galaxies, which then evolve into quasars as the dust and gas are blown out by the AGN activity. This fueling episode might correspond to a high Eddington fraction.

BALQSOs such as PG 1700+518 might then be characterized as young or recently refueled quasars. Boroson & Meyers (1992) noted that low-ionization BALQSOs constitute 10% of IR-selected quasars (not the 1% of optically selected

quasars), and that they show very weak narrow [O III] $\lambda 5007$ emission, and, in an HST survey, Turnshek et al. (1997) find that 1/3 of weak [O III] $\lambda 5007$ quasar show BALs. Voit et al. (1993) argue that low-ionization BALs are a manifestation of a “quasar’s efforts to expel a thick shroud of gas and dust.” All of the low-ionization BALQSOs in Figure 2 lie at the extreme low [O III] $\lambda 5007$, high Fe II corner. PG 1700+518 shows evidence for a recent interaction: a nuclear starburst ring (Hines et al. 1998) and a companion galaxy with a 100 million year old starburst (Stockton et al. 1998).

Such an environment with a high covering factor of high density/column density clouds can quench or frustrate radio jets (at least for certain models of jets), which would explain the anti-correlation between the presence of BALs and radio power (Stoche et al. 1992; Brotherton et al. 1998) and the association of radio-loud quasars with strong NLR and ILR emission (Fig. 2; Francis, Hooper, & Impey 1993).

5. Application to the Baldwin Effect

Even without a physical explanation for eigenvector 1, the relationships can be used empirically. In the investigations of Wills et al. (1993) and Brotherton et al. (1994a), C IV $\lambda 1549$ did not display a significant Baldwin effect. These samples covered only a small range in quasar luminosity. The EW_{CIV} strongly correlated with $FWHM_{CIV}$, suggesting eigenvector 1 to be the source of scatter in the Baldwin effect. Multiple regression using both EW_{CIV} and $FWHM_{CIV}$ as predictors of luminosity should produce a tightened Baldwin effect if this hypothesis is true.

The Large Bright Quasar Survey or LBQS (Hewett et al. 1995) is the largest complete optically selected sample anyone has yet studied in detail (although the luminosity range is relatively small). Francis et al. (1992) measured the Baldwin effect for a high-redshift subsample of the LBQS, both for the entire C IV $\lambda 1549$ line and also the line core and line wings separately. They found marginally significant differences suggesting that the line cores contributed most to the effect.

Figure 3 shows data from the LBQS investigation by Francis et al. (1992), with an addition: a vector showing the magnitude and direction of eigenvector 1 (from their spectral PCA) for each quasar. The distribution does not appear independent of luminosity: the left part of the plot is heavy with up vectors, the right side with down vectors. Eigenvector 1 is a primary cause of the Baldwin effect in this sample. Correcting for eigenvector 1 would not reduce the Baldwin effect scatter, but the Baldwin effect itself.

Osmer, Porter, & Green (1994) created composite spectra for samples of quasars with different luminosities. Difference spectra showed that the change in emission-line equivalent width was confined to the low-velocity gas.

Unfortunately the situation appears to be different at low luminosities. Boroson & Green (1992) identify luminosity with eigenvector 2 in their PCA of the BQS. Wills et al. (this volume) also identifies luminosity and the Baldwin effect with an eigenvector 2. The luminosity ranges of these samples are again not ideal for investigating the Baldwin effect.

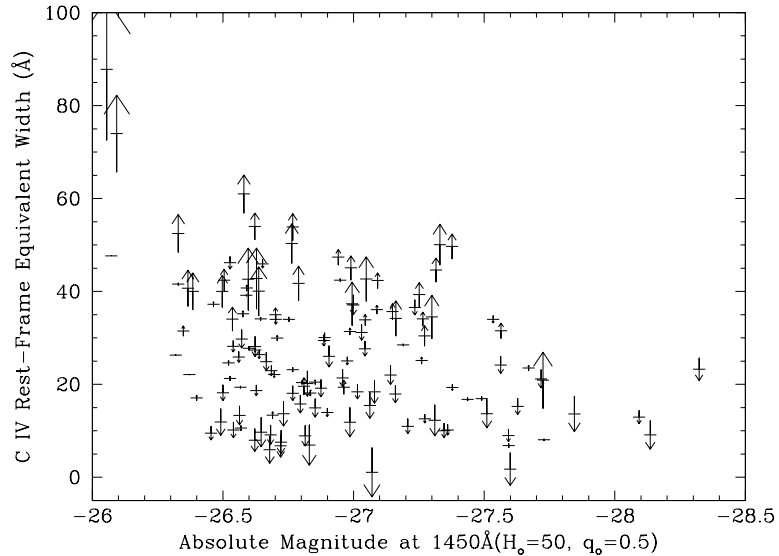


Figure 3. The Baldwin effect in the LBQS sample from Francis et al. (1992). The arrows on each point indicate the value of principal component 1 (PC1) from their spectral principal component analysis. Large up arrows indicate narrow peaky C IV lines, and large down arrows indicate broad, flat-topped profiles. The fact that the distribution of PC1 weights changes with luminosity suggests that its variation also drives the Baldwin effect.

6. Conclusions and Future Directions

There is conflicting evidence about whether or not eigenvector 1 correlations are driving the Baldwin effect or driving scatter in the Baldwin effect. The answer is of course high-quality data on a large carefully selected sample covering a wide range of luminosity, followed by multivariate analysis. An appropriate data set does not as yet appear to exist.

Acknowledgments. I would like to thank Bev Wills for her contributions, both tangible and intangible. This work has been performed under the auspices of the U.S. Department of Energy by Lawrence Livermore National Laboratory under Contract W-7405-ENG-48.

References

- Baker, J. C. 1997, MNRAS, 286, 23
- Baldwin, J. A., & Netzer, H. 1978, ApJ, 226, 1
- Baldwin, J., Ferland, G., Korista, K., & Verner, D. 1995, ApJ, 455, L119
- Bernstein, I. H. 1988, Applied Multivariate Analysis (New York: Springer-Verlag), chapter 6
- Boroson, T. A., & Green, R. F. 1992, ApJS, 80, 109
- Boroson, T. A. & Meyers, K. A. 1992, ApJ, 397, 442

Brotherton, M. S. 1996a, *ApJS*, 102, 1
 Brotherton, M. S. 1996b, PhD Thesis, Univ. of Texas at Austin
 Brotherton, M. S., et al. 1998, *ApJ*, 505, L7
 Brotherton, M. S., Wills, B. J., Steidel, C. C., & Sargent, W. L. W. 1994a, *ApJ*, 423, 131
 Brotherton, M. S., Wills, B. J., Francis, P. J., & Steidel, C. C. 1994b, *ApJ*, 430, 495
 Collin-Souffrin, S., Hameury, J. -M., & Joly, M. 1988, *A&A*, 205, 19
 Corbin, M. 1993, *ApJ*, 403, L9
 Espey, B. R., Carswell, R. F., Bailey, J. A., Smith, M. G., & Ward, M. J. 1989, *ApJ*, 342, 666
 Espey, B. R., et al. 1994, *ApJ*, 434, 484
 Ferland, G. J. 1987, in *Rutherford-Appleton Workshop on Emission Lines in AGN*, ed. P. M. Gondhalekar (RAL-87-109), 109
 Ferland, G. J. 1993, University of Kentucky Department of Physics and Astronomy Internal Report
 Francis, P. J., Hewitt, P. C., Foltz, C. B., & Chaffee, F. H. 1992, *ApJ*, 398, 476
 Francis, P. J., Hooper, E. J., & Impey, 1993, *AJ*, 106, 417
 Gaskell, C. M. 1982, *ApJ*, 263, 79
 Ghisellini, G., George, I. M., Fabian, A. C., & Done, C. 1991, *MNRAS*, 248, 14
 Green, P. J. 1998, *ApJ*, 498, 170
 Hewett, P. C., Foltz, C. B., & Chaffee, F. H. 1995, *AJ*, 109, 1498
 Hines, D., et al. 1997, *BAAS*, 191, 113008
 Jackson, N., & Browne, I. W. A. 1991, *MNRAS*, 250, 422
 Jackson, N., Browne, I. W. A., Murphy, D. W., & Saikia, D. J. 1989, *Nature*, 338, 485
 Kaspi, S., Smith, P. S., Maoz, D., Netzer, H., & Jannuzi, B. T. 1996, *ApJ*, 471, L75
 Korista, K. et al. 1995, *ApJS*, 97, 285
 Kwan, J., & Krolik, J. H. 1981, *ApJ*, 250, 478
 Kwan, J, Cheng, F, Fang, L., Zheng, W, Ge, J. 1995, *ApJ*, 440, 628
 Laor, A., Fiore, F., Elvis, M., Wilkes, B. J., & McDowell, J. C. 1997, *ApJ*, 477, 93
 Laor, A., Fabrizio, F., Elvis, M., Wilkes, B. J., & McDowell, J. C. 1994, *ApJ*, 435, 611
 Marziani, P., Sulentic, J. W., Dultzin-Hacyan, D., Calvani, M., & Moles, M. 1996, *ApJS*, 104, 37
 Mushotsky, R. F., & Ferland, G. J. 1984, *ApJ*, 278, 558
 Netzer, H. 1985, *MNRAS*, 216, 63
 Netzer, H., et al. 1994, *ApJ*, 430, 191
 Orr, M. J. L., & Browne, I. W. A. 1982, *MNRAS*, 200, 1067
 Osmer, P. S., Porter, A. C., & Green, R. F. 1994, *ApJ*, 436, 678

- Pounds, K. A., Done, C., Osborne, J. P. MNRAS, 277, L5
- Sanders, D. B., Soifer, B. T., Elias, J. H., Neugebauer, G., & Matthews, K. 1988, ApJ, 328, L35
- Stočke, J. T., Morris, S. L., Weymann, R. J., & Foltz, C. B. 1992, ApJ, 396, 487
- Stockton, A., Canalizo, G., & Close, L. M. 1998, ApJ, 500, L121
- Turnshek, D. A., Monier, E. M., Sirola, C. J., & Espey, B. R. 1997, ApJ, 476, 40
- Voit, G. M., Weymann, R. J., & Korista, K. T. 1993, ApJ, 95, 109
- Wandel, A., & Boller, T. 1998, A&A, 331, 884
- Wang, T., Zhou, Y., & Gao, A. 1996, ApJ, 457, 111
- White, N. E., Fabian, A. C., & Mushotzky, R. F. 1984, A&A, 133, L9
- Wills, B. J., Brotherton, M. S., Fang, D., Steidel, C. C., & Sargent, W. L. W. 1993, ApJ, 415, 563
- Wills, B. J., & Brotherton, M. S. 1995, ApJ, 448, L81
- Wills, B. J., & Brotherton, M. S. 1996, in *Jets from Stars and AGN*, ed. Kundt (New York: Springer-Verlag), 203
- Wills, B. J., & Browne, I. W. A. 1986, ApJ, 302, 56
- Zheng, W., & O'Brien, P. 1990, ApJ, 353, 433